Ultrasound irradiation inhibits proliferation of cervical cancer cells by initiating endoplasmic reticulum stress-mediated apoptosis and triggering phosphorylation of JNK

Juan Qin[1,B–D,F], Guolin Song[2,B–D,F], Yan Wang[3,A,B,E,F], Qin Liu[1,B,C,E,F], Hong Lin[1,B,C,F], Jinyun Chen[3,A,C,E,F]

[1] Department of Gynecology, Guiyang Maternal and Child Health Care Hospital, China
[2] Guizhou University of Traditional Chinese Medicine, Guiyang, China
[3] State Key Laboratory of Ultrasound in Medicine and Engineering, College of Biomedical Engineering, Chongqing Key Laboratory of Biomedical Engineering, Chongqing Medical University, China

A – research concept and design; B – collection and/or assembly of data; C – data analysis and interpretation; D – writing the article; E – critical revision of the article; F – final approval of the article

Advances in Clinical and Experimental Medicine, ISSN 1899–5276 (print), ISSN 2451–2680 (online) *Adv Clin Exp Med*. 2021;30(5):545–554

Address for correspondence
Jinyun Chen
E-mail: qinjuan2019@sina.com

Funding sources
National Natural Science Foundation (grant No. 81860328) and Guizhou Provincial Science and Technology Foundation [2013] 2020.

Conflict of interest
None declared

Received on June 28, 2020
Reviewed on October 4, 2020
Accepted on February 19, 2021

Published online on May 18, 2021

Cite as
Qin J, Song G, Liu Q, Lin H, Wang Y, Chen J. Ultrasound irradiation inhibits proliferation of cervical cancer cells by initiating endoplasmic reticulum stress-mediated apoptosis and triggering phosphorylation of JNK. *Adv Clin Exp Med*. 2021;30(5):545–554. doi:10.17219/acem/133488

DOI
10.17219/acem/133488

Abstract

Background. Cervical cancer is the 2nd most frequently diagnosed gynecological cancer. Therefore, it is clinically significant to discover an effective anti-cancer approach.

Objectives. This study aimed to investigate the effects of low-intensity ultrasound irradiation (USI) on cervical cancer cells and associated mechanisms of cell death.

Materials and methods. Normal human cervical HaCaT cells and cervical cancer cell lines C33A, Hela and Siha were cultured and γ-rays applied at a dosage of 2.0 Gy/min. The MTT assay was then used to assess viability (proliferation) of HaCaT, C33A, Hela, and Siha cells. Small interfering RNA (siRNA) sequences that silence the glucose-related protein (*GRP78*) gene were synthesized. Structural changes to cells exposed to USI were observed with scanning electron microscopy. Immunocytochemistry and western blotting were utilized to examine *GRP78*, C/EBP-homologous protein (CHOP), phosphorylated JNK (p-JNK), and caspase-12 expression in cervical cancer cells.

Results. Ultrasound irradiation reduced the viability of cervical cancer cells and increased apoptosis, compared to untreated tumor cells ($p < 0.05$). This effect was not apparent on HaCaT cells. Ultrasound irradiation also induced formation of apoptotic bodies compared to untreated tumor cells ($p < 0.05$), and activated endoplasmic reticulum (ER) stress-associated apoptosis compared to untreated tumor cells ($p < 0.05$), by triggering *GRP78*, CHOP and caspase-12 expression. Moreover, USI triggered ER stress by upregulating *GRP78* expression. Remarkably, USI triggered phosphorylation of JNK compared to untreated tumor cells ($p < 0.05$). Ultrasound irradiation initiated phosphorylation of JNK by increasing *GRP78* expression. Silencing of *GRP78* further enhanced the effect of USI on tumor cells.

Conclusions. Ultrasound irradiation significantly inhibited proliferation and induced apoptosis of cervical cancer cells by initiating ER stress associated with apoptosis signaling pathways and triggering phosphorylation of JNK.

Key words: apoptosis, cervical cancer, ER stress, ultrasound irradiation

Background

Cervical cancer is the 2nd most frequently diagnosed gynecological cancer and the 4th leading cause of tumor-associated death for females worldwide.[1,2] About 275,100 women are diagnosed with cervical cancer and die every year, which accounts for 9% of all cancer-associated female mortality.[3] Among the deaths from cervical cancer, approx. 85% occurs in developing countries,[4] where patients lack the effective therapy resources for cervical cancer treatment. Therefore, it is clinically significant to discover an effective anti-cancer approach and clarify the associated mechanisms of cervical cancer proliferation.

According to previous investigations,[5,6] non-invasive surgery for cancer treatment that induces cancer cell apoptosis, is an effective approach for killing the cancer cells. In recent years, ultrasound irradiation (USI) has been proven to induce apoptosis of some tumor cell lines, such as human leukemia, ovarian carcinoma and lung cancer cells.[7–9] Actually, low-intensity USI exhibits great potential to induce apoptosis as it is easily applied, and therefore should be considered to be the optimal ultrasound for cancer treatment in clinic.[10] As low-intensity USI triggers apoptosis in various cancers, it could be employed as a promising strategy to eliminate tumor cells.[11] Meanwhile, a study by Yang et al.[12] also reported that USI induced apoptosis in numerous cancer cells by activating different apoptotic signaling pathways, including endoplasmic reticulum (ER) stress-associated and mitochondrial pathways.

Objectives

By considering the potential effects of USI on cancer cell apoptosis, we hypothesized that the USI treatment might play a critical role for inducing cervical cancer cell apoptosis. Thus, the present research aimed to clarify the effects of low-intensity USI on apoptosis of cervical cancer cell lines and the apoptosis-associated mechanisms.

Materials and methods

Cell culture

The human normal cervical cell line (HaCaT) and the cervical cancer cell lines C33A, Hela and Siha were cultured in Dulbecco's modified Eagle's medium (DMEM; Gibco, Grand Island, USA) supplemented with 10% fetal bovine serum (FBS; Gibco) and 1% penicillin-streptomycin (Beyotime, Shanghai, China) in the humidified atmosphere with 5% CO_2 at 37°C.

Ultrasound irradiation administration and trial grouping

The C33A, Hela and Siha groups were subdivided into HaCaT group (only referring to the MTT and flow cytometry assay), untreated tumor cells (i.e., tumor cells not treated with USI) group, tumor cells exposed to USI and then cultured for 6 h (6 h group), tumor cells exposed to USI and then cultured for 12 h (12 h group), and tumor cells exposed to USI and then cultured for 24 h (24 h group). The USI was conducted using the JC200 Haifu ultrasound system (Chongqing Haifu Medical Technology Co. Ltd., Chongqing, China). The USI processes were assigned based on a previous study.[13] Cells were treated with USI at a transducer frequency of 10.0 MHz and with mechanical index (power) of 0.25 W/cm^2 for 10 s.

MTT assay

Suspensions of HaCaT, C33A, Hela, and Siha cells were seeded into 96-well cell culture plates (Corning-Costar, Corning, USA) at a dosage of 1×10^6 cells/mL and cultured for 6–24 h at 37°C. In order to evaluate the cell viability (cell proliferation), 20 µL of MTT solution (5 mg/mL in phosphate-buffered saline (PBS; Beyotime) was added to each well and cultured for another 4 h at 37°C. After the incubation of MTT, a total of 200 µL of dimethyl sulfoxide (DMSO; Amresco Inc., Solon, USA) was added to the wells for 10 min to dissolve any formed formazan crystals. Finally, the absorbance of each well was examined at wavelength of 490 nm using a Multiskan Mk3 microplate reader (Thermo Scientific Pierce, Shanghai, China).

Flow cytometry assay

Apoptosis of cervical cancer cells, including HaCaT, C33A, Hela, and Siha, were assessed with Annexin V-PE/7-AAD Apoptosis Detection regent (Cat. No. 559763; Becton Dickinson Biosciences, San Jose, USA) based on the manufacturer's protocol. Briefly, cells were collected and treated with Annexin V-PE for 15 min and then propidium iodide (PI) for 15 min in the dark at 25°C. Next, cells were analyzed using a FACS Vantage SE (Becton Dickinson Biosciences) flow cytometer, using the 546/647 band-pass filter (for monitoring PI signals) and the 530/578 band-pass filter (for monitoring Annexin-V signals), and the data were analyzed with the Cell Quest software v. 5.1 (Becton Dickinson Biosciences).

Small interfering RNA synthesis and identification

The Small interfering RNA (siRNA) synthesis was conducted according to a previous study.[14] The candidate sequences for the siRNA synthesis, and the optimal siRNA sequences for silencing the glucose-related protein

Table 1. siRNA sequences for *GRP78* gene silencing and primer for PCR assay

Genes or siRNAs	Sense/anti-sense	Sequences
GRP78-homo-731	sense	5′-GAGGCUUAUUUGGGAAAGATT-3′
	anti-sense	5′-UCUUUCCCAAAUAAGCCUCTT-3′
GRP78-homo-1081	sense	5′-GGGCAAAGAUGUCAGGAAATT-3′
	anti-sense	5′-UUUCCUGACAUCUUUGCCCTT-3′
GRP78-homo-1548	sense	5′-GAGGUGUCAUGACCAAACUTT-3′
	anti-sense	5′-AGUUUGGUCAUGACACCUCTT-3′
Negative control	sense	5′UUCUCCGAACGUGUCACGUTT-3′
	anti-sense	5′-ACGUGACACGUUCGGAGAATT-3′
GRP78	forward	5′-AGACGGGCAAAGATGTCAGG-3′
	reverse	5′-GAGTCGAGCCACCAACAAGA-3′

(*GRP78*) gene identified using quantitative real-time polymerase chain reaction (qRT-PCR) analysis with specific primer for *GRP78* are listed in Table 1. The siRNA was transfected into the above cell lines using Lipofectamine 2000 regent (Invitrogen/Life Technologies, Carlsbad, USA). Briefly, RNAs in all tumor cells were extracted using Trizol kits (Beyotime). Complementary DNAs (cDNAs) were then synthesized with the cDNA Synthesis Kit (Cat. No. 18080200; Thermo Fisher Scientific, Rockford, USA) following the manufacturer's protocol. The mRNA levels of *GRP78* gene were determined with SYBR-Green I PCR system, purchased from Western Biotech (Chongqing, China), using specific primers (Table 1). Amplified products for *GRP78* gene were analyzed using GDS8000 Gel-Scanning equipment (UVP, Sacramento, USA) based on equipment instructions. Finally, the *GRP78* gene expression was calculated and analyzed using $2^{-\Delta\Delta ct}$ method.

Scanning electron microscopy

The structural changes of the cervical cancer cells when exposed to USI were observed using scanning electron microscopy. Briefly, cervical cancer cells were adjusted to the concentration of 10^6 cells/well on six-well plates and cultured for 24 h to confirm adhesion. Cells were washed with PBS and the suspensions were dropped onto glass coverslips for 30 min and then incubated using 4% formalin (Beyotime) for 5 min. Then, cells were fixed using the 1% osmic acid (Beyotime) for 30 min, washed with ice-cold PBS solution and then soaked in 2% tannin (Beyotime) overnight at 4°C. Finally, cervical cancer cells were coated with a vacuum spray-plating equipment and the image was captured using scanning electron microscope S-3000N (Hitachi, Tokyo, Japan).

Immunocytochemistry assay

All cells were cultured onto slides and fixed with 4% paraformaldehyde (Beyotime) at room temperature for 10 min. Cells were washed with PBS and endogenous peroxidase inactivated using 3% hydrogen peroxide (Beyotime) at 25°C for 5 min. Cells were subsequently blocked using 5% bovine serum albumin solution (BSA; Beyotime) at 25°C for 15 min, then incubated with rabbit anti-human *GRP78* monoclonal antibody (1 : 3000, Cat. No. ab108615; Abcam, Cambridge, USA), rabbit anti-human C/EBP-homologous protein (CHOP) polyclonal antibody (1 : 3000, Cat. No. MBS000292; MyBioSource, Vancouver, Canada), rabbit anti-human phosphorylated C-Jun N-terminal kinase (p-JNK) monoclonal antibody (1 : 3000, Cat. No. ab124956; Abcam), and rabbit anti-human caspase-12 polyclonal antibody (1 : 2000, Cat. No. ab62484; Abcam) overnight at 4°C. Subsequently, cells were washed using PBS and incubated using Biotin-labeled goat anti-rabbit antibody (1 : 1000, Cat. No. ab6720; Abcam) for 60 min at 37°C. Finally, cells were observed and images captured using a professional CKX41 inverted fluorescence microscope (Olympus Corp., Tokyo, Japan).

Western blot assay

The cervical cancer cells were lysed with RIPA buffer (Beyotime) according to manufacturer's protocol. Cell lysates were then separated using 15% SDS-PAGE (Beyotime) and electrotransferred onto polyvinylidene fluoride (PVDF) membranes (Bio-Rad, Hercules, USA). The membrane was blocked using PBS solution containing 5% skim milk and supplementing with 0.05% Tween-20 (Beyotime). Subsequently, PVDF membrane was treated with rabbit anti-human *GRP78* monoclonal antibody (1 : 3000; Abcam), rabbit anti-human CHOP polyclonal antibody (1 : 2000; MyBioSource), rabbit anti-human p-JNK monoclonal antibody (1 : 3000; Abcam), rabbit anti-human caspase-12 polyclonal antibody (1 : 2000; Abcam), and rabbit anti-human β-actin polyclonal antibody (1 : 2000; Abcam) overnight at 4°C. Subsequently, PVDF membranes were treated with horseradish peroxidase (HRP)-labeled goat anti-rabbit antibody (1 : 2000; Abcam). The western blot band signals for the isolated proteins were visualized and imaged with ECL Western Blotting Substrate (Cat. No. 32106, Thermo

Fisher Scientific). Finally, the images were captured using GDS8000 Gel Scanning System (UVP).

Statistical analyses

Our data were analyzed using IBM SPSS v. 19.0 software (IBM Corp., Armonk, USA). All data are presented as mean ± standard deviation (SD). The statistical differences between 2 groups were analyzed using the Student's t test. The differences among multiple groups were also analyzed using the Tukey's post hoc test-validated analysis of variance (ANOVA). A p-value <0.05 represented a significant difference. At least 6 repeats were conducted for all tests or experiments.

Results

Ultrasound irradiation reduced viability and increased apoptosis of cervical cells

In order to observe effects of USI on the proliferation of HaCaT, C33A cells, Hela cells, and Siha cells, an MTT assay was conducted. The MTT results indicated that cell viabilities were significantly reduced at 6 h, 12 h and 24 h post-treatment compared with the untreated cells (Fig. 1A, $p < 0.05$). Meanwhile, the apoptosis of cervical cancer cells was measured with flow cytometry. Our findings showed that cell apoptosis rates were significantly increased at 6 h, 12 h and 24 h post-treatment compared with untreated cells (Fig. 1B, $p < 0.05$).

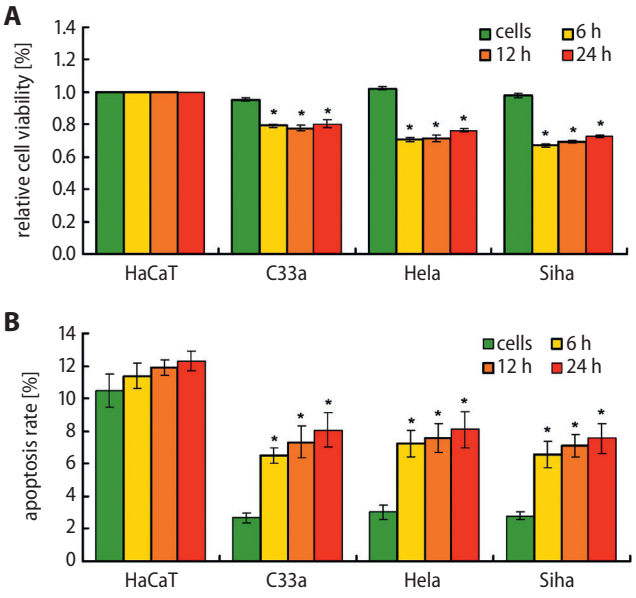

Fig. 1. Evaluation for cell viability and cell apoptosis of normal cervical cells and cervical cancer cells. A. Statistical analysis for cell viability of normal cervical cell (HaCaT) and cervical cancer cell lines C33A, Hela and Siha cells at 6 h, 12 h and 24 h post-USI; B. Statistical analysis for cell apoptosis of normal cervical cell HaCaT and cervical cancer cell lines C33A, Hela and Siha cells at 6 h, 12 h and 24 h post-USI

*$p < 0.05$ compared to untreated cells (HaCaT, C33A, Hela, and Siha).

Ultrasound irradiation induced the formation of apoptotic body

To confirm the reason that USI caused cervical cancer cell death, apoptotic bodies were evaluated in Hela cells. The results indicated that there were no apoptotic bodies present in the untreated cells (Hela cells) (Fig. 2). However, apoptotic bodies in the 6-hours treatment group and 12-hours treatment group were visibly more compared to that in untreated cells (Fig. 2). Meanwhile, both C33A and Siha cells displayed numerous apoptotic bodies (data not shown).

Ultrasound irradiation activated ER stress-associated apoptosis

The ER stress-associated apoptotic signaling molecules,[15] including *GRP78*, CHOP and caspase-12, were examined with immunocytochemistry analysis. Our findings demonstrated that USI significantly increased caspase-12 expression in C33A cells, Hela cells and Siha cells, compared with the untreated cells (Fig. 3, $p < 0.05$). Furthermore, USI significantly upregulated CHOP expression in C33A cells, Hela cells and Siha cells, compared with the untreated cells (Fig. 4, $p < 0.05$). Finally, compared with the untreated cells, *GRP78* levels were also significantly enhanced in the C33A cells, Hela cells and Siha cells undergoing the USI treatment (Fig. 5, $p < 0.05$).

Ultrasound irradiation increased phosphorylation of JNK

The phosphorylation of the JNK molecule could reflect apoptosis occurring within cancer cells. Therefore, we examined the expression of p-JNK in C33A, Hela and Siha cells. The present findings showed that USI significantly increased phosphorylation of JNK in both C33A and Siha cells, compared to that in the untreated tumor cells at 6 h, 12 h and 24 h post-treatment (Fig. 6, $p < 0.05$). However, the effects of USI on p-JNK were not found in Hela cells (Fig. 6).

Ultrasound irradiation triggered ER stress by modulating *GRP78* expression

In this study, we synthesized 3 siRNA sequences, and found that the siRNA sequence *GRP78*-homo-1548 exhibited the best silencing effects on *GRP78* expression (Fig. 7), and was therefore used for subsequent studies in cervical cancer cells.

To determine specific mechanisms associated with USI-triggered ER stress, the stress-regulatory protein *GRP78* was detected with western blotting analysis (Fig. 8A). Our findings demonstrated that USI significantly increased caspase-12 (Fig. 8B), CHOP (Fig. 8C) and *GRP78* (Fig. 8D) protein expression in Hela cells at all time points

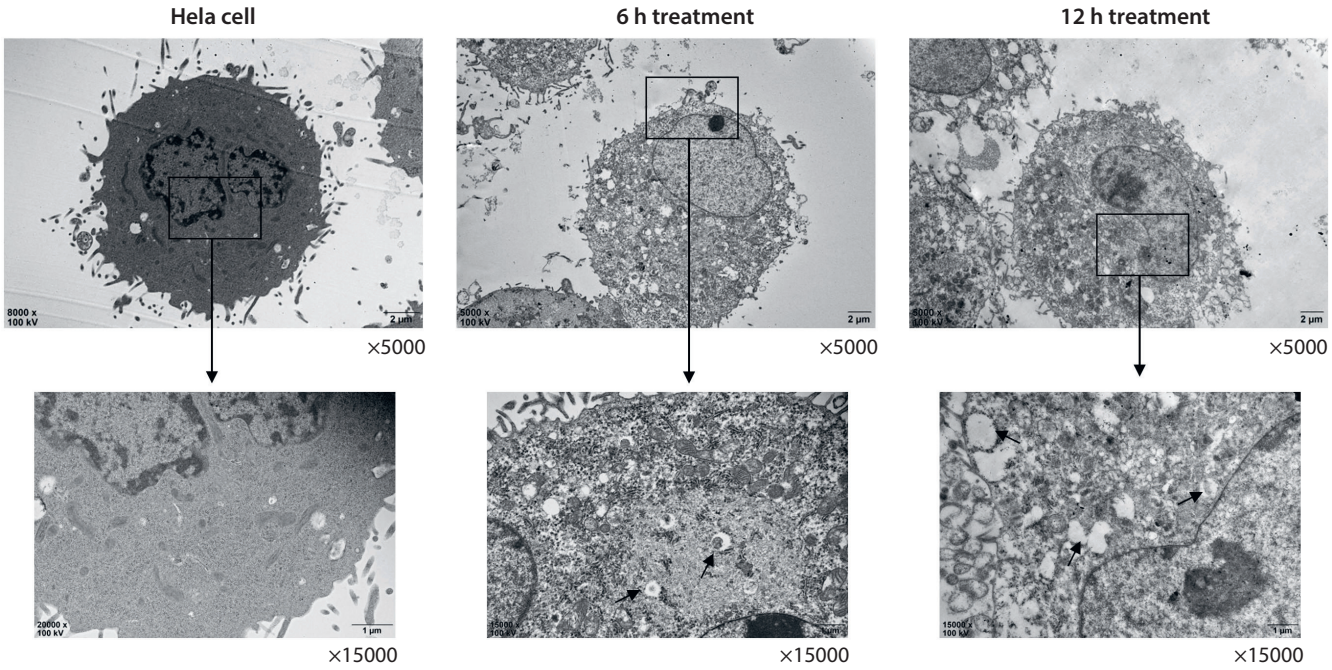

Fig. 2. Observation of structural changes of normal cervical cells and cervical cancer cells exposed to USI using scanning electron microscopy. The black arrows represent the apoptotic bodies

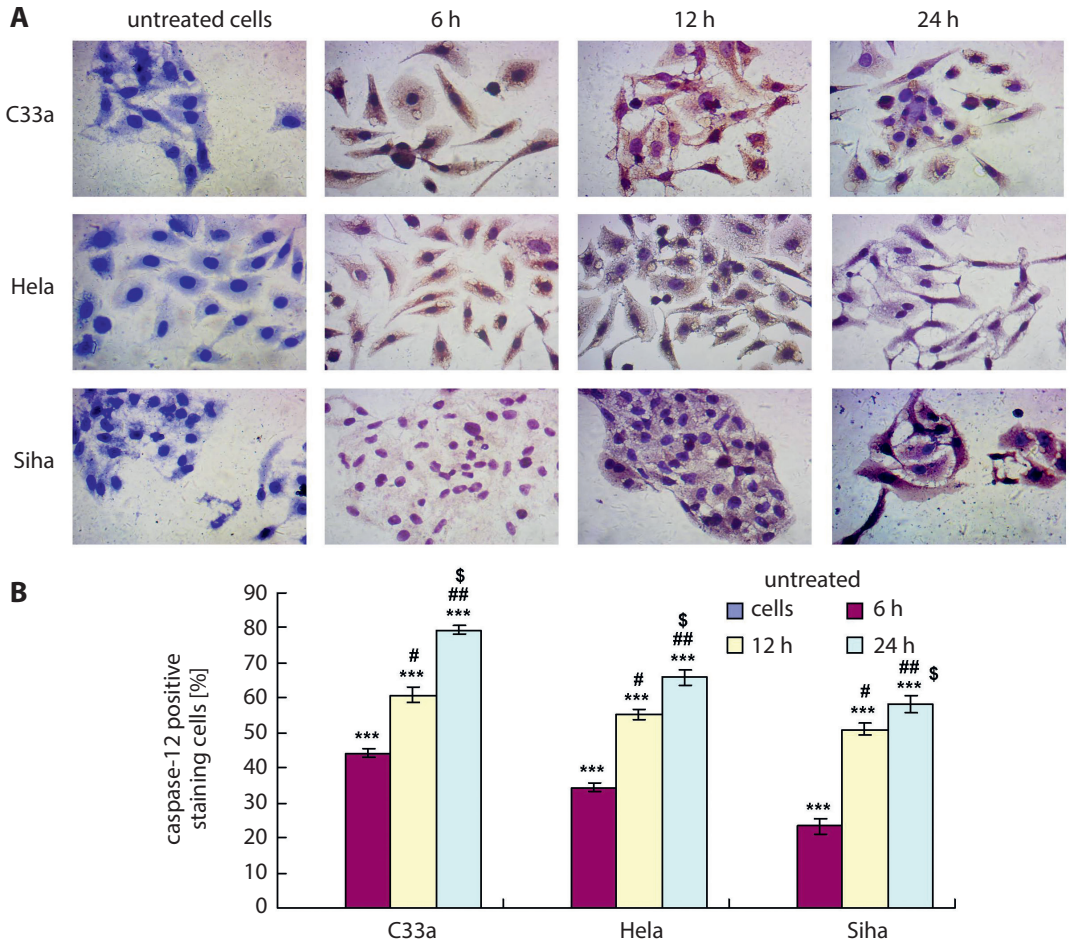

Fig. 3. Examination for caspase-12 expression in cervical cancer cells using immunocytochemistry assay. A. Immunocytochemistry images of caspase-12 expression in C33A, Hela and Siha cells; B. Statistical analysis of the expression of caspase-12 in cells; ×200 magnification

***p < 0.001 compared to untreated cells; #p < 0.05 and ##p < 0.01 compared to 6 h USI administration group; $p < 0.05 compared to 12 h USI administration group.

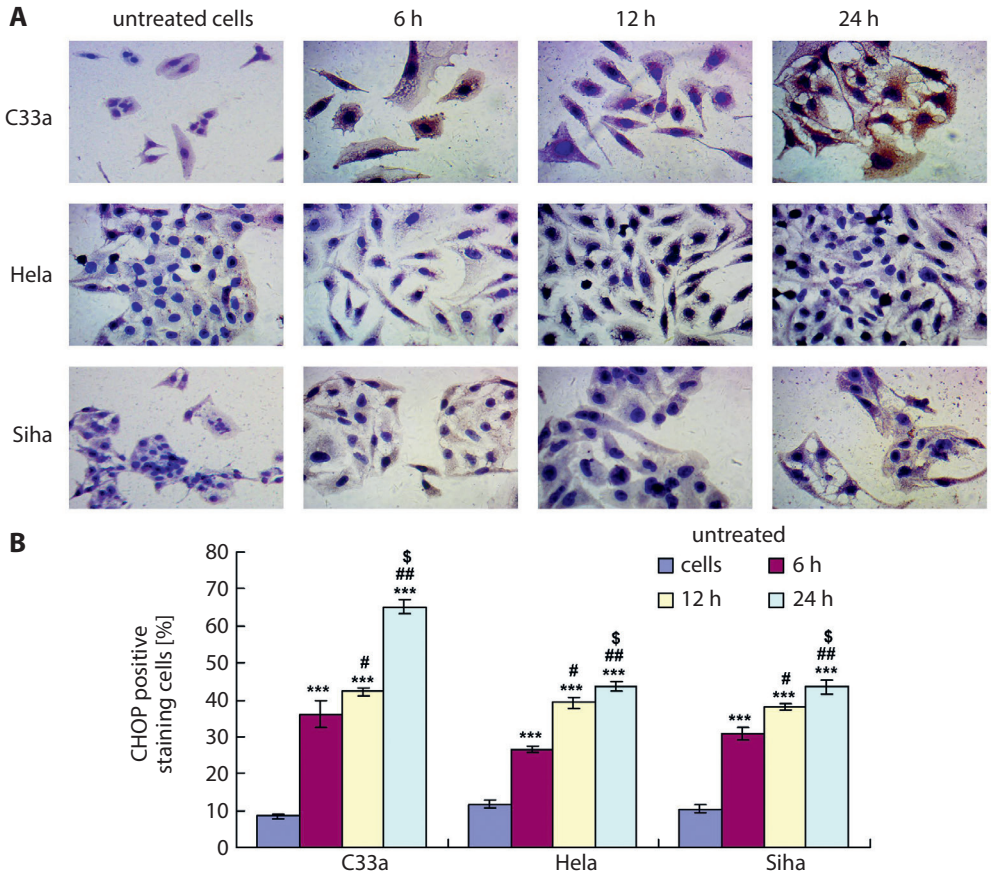

Fig. 4. Evaluation of CHOP expression in cervical cancer cells with immunohistochemistry assay. A. Immunohistochemistry images for CHOP expression in C33A, Hela and Siha cells; B. Statistical analysis of the CHOP expression in cells; ×200 magnification

***p < 0.001 compared to untreated cells group; #p < 0.05 and ##p < 0.01 compared to 6 h USI administration group; $p < 0.05 compared to 12 h USI administration group.

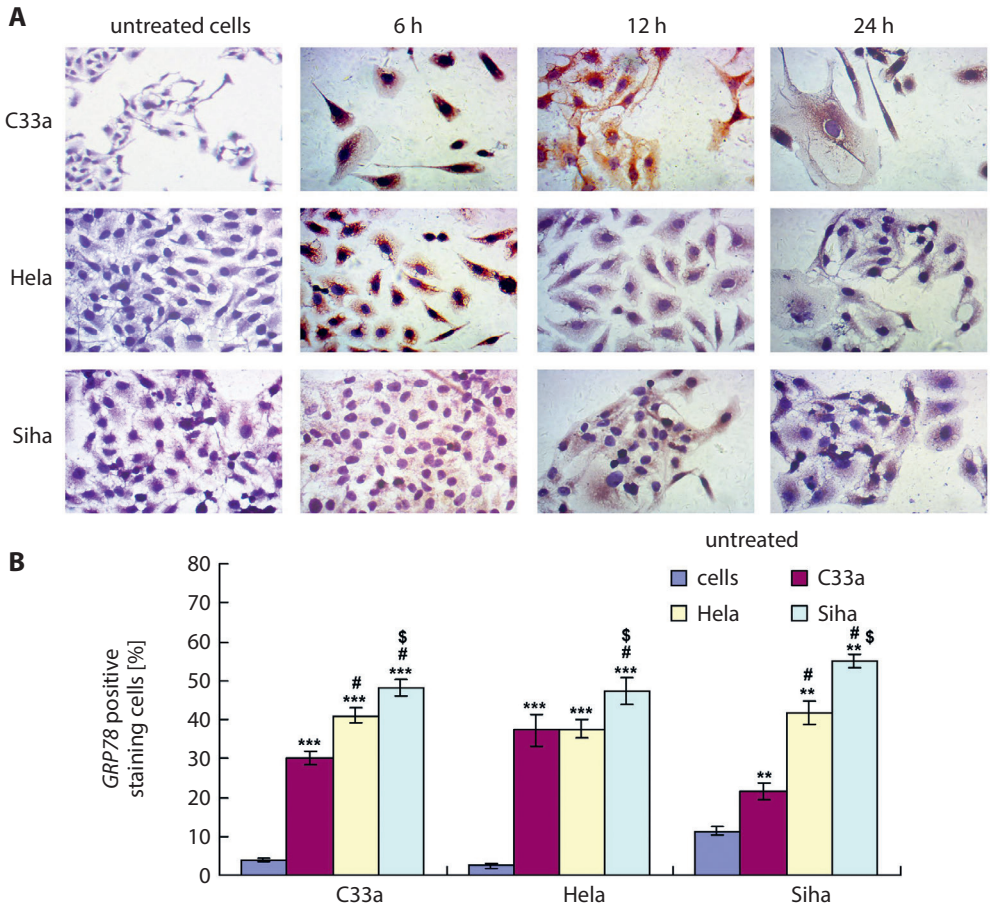

Fig. 5. Determination of *GRP78* expression in cervical cancer cells with immunohistochemistry analysis. A. The images for the immunohistochemistry assay for expression of *GRP78* in C33A, Hela and Siha cells; B. Statistical analysis for expression of *GRP78* in cells; ×200 magnification

**p < 0.01 and ***p < 0.001 compared to untreated cells group; #p < 0.05 compared to 6 h USI administration group; $p < 0.05 compared to 12 h USI administration group.

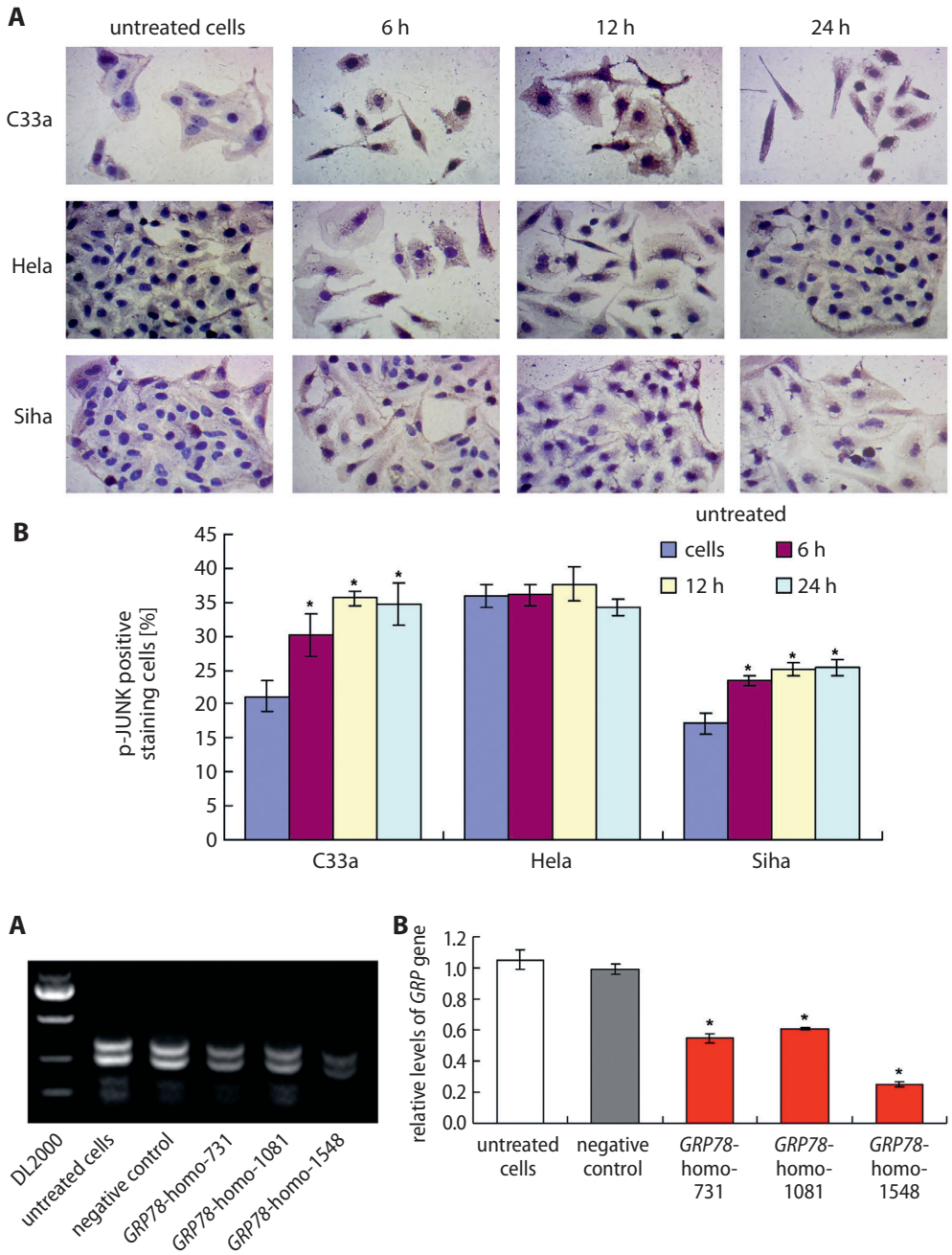

Fig. 6. Determination for *GRP78* expression in cervical cancer cells with the immunohistochemistry analysis. A. The images for the immunohistochemistry for expression of *GRP78* in C33A, Hela and Siha cells; B. Statistical analysis of the expression of *GRP78* in cells; ×200 magnification

*p < 0.05 compared to untreated cells group.

Fig. 7. Identification and screening for *GRP78* silencing siRNA sequences. A. Gel image for the *GRP78* siRNA sequences; B. Statistical analysis for the levels of GRP sequences

*p < 0.05 compared to untreated cells group.

post-treatment, compared to that of the untreated cells ($p < 0.05$). Meanwhile, inhibition of *GRP78* (siRNA treatment) also significantly enhanced the expression of caspase-12 (Fig. 8B, 12 h post-USI administration), CHOP (Fig. 8C, at 6 h, 12 h and 24 h post-USI treatment) and reduced GRP78 (Fig. 8D, at 6 h, 12 h and 24 h post-USI treatment) proteins in Hela cells compared to that in the untreated tumor cells ($p < 0.05$) at 6 h, 12 h and 24 h post-USI treatment.

Finally, suppression of *GRP78* also significantly increased the expression of caspase-12, CHOP and decreased GRP78 proteins in C33A and Siha cells compared to that in the untreated tumor cells at 6 h, 12 h and 24 h post-treatment (data not shown).

Ultrasound irradiation enhanced phosphorylation of JNK by downregulating *GRP78* expression

The results showed that suppression of *GRP78* enhanced the ratio of JNK p-JNK/JNK in Hela cells compared to that in the untreated tumor cells at 6 h, 12 h and 24 h post-treatment (Fig. 8E, $p < 0.05$). Moreover, inhibition of *GRP78* also significantly increased expression of p-JNK in C33A cells and Siha cells compared to that in untreated tumor cells (data not shown).

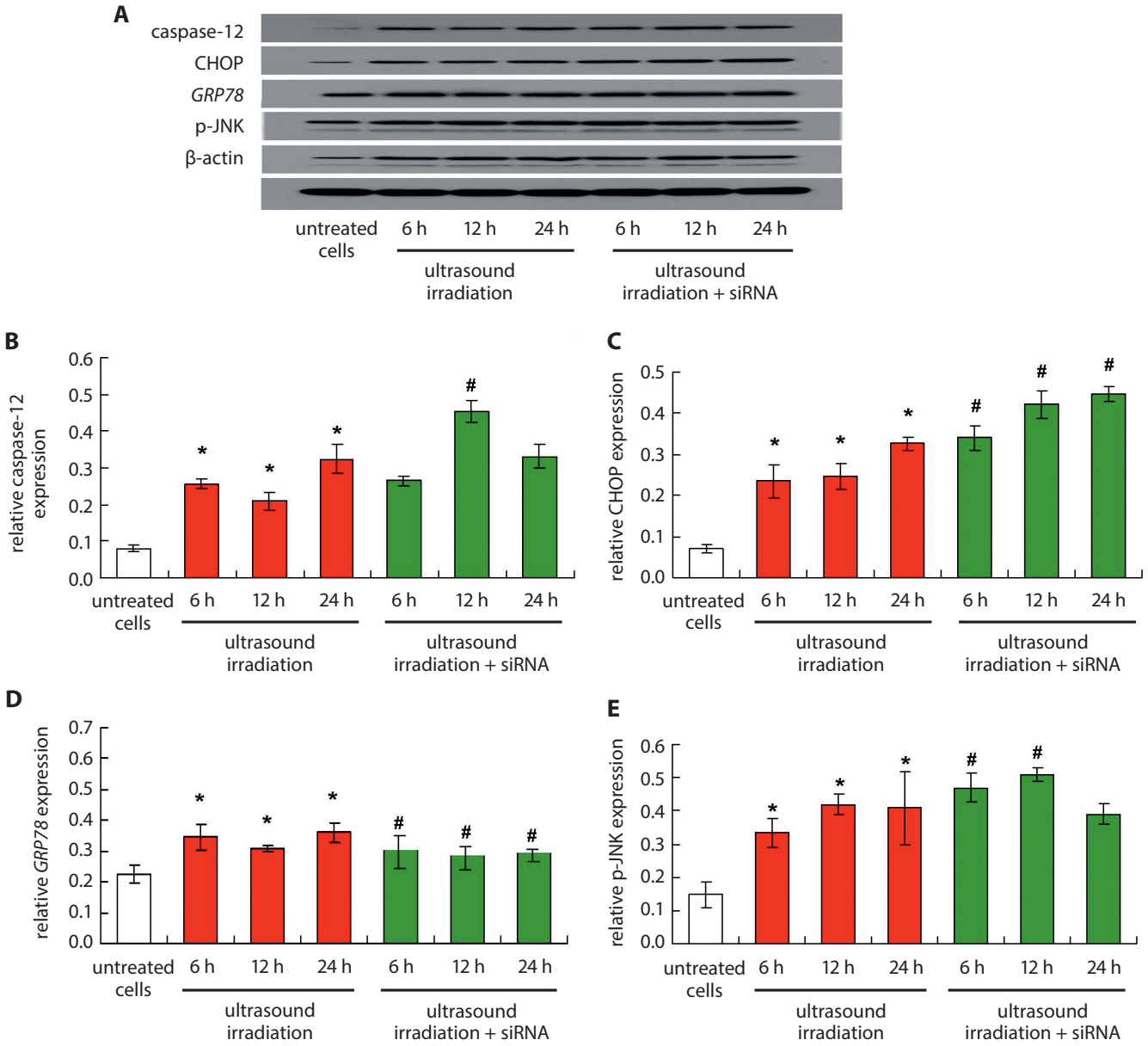

Fig. 8. Evaluation for caspase-12, CHOP, *GRP78*, and p-JNK expression in cervical cancer cells using western blotting assay. A. Images of western blotting assays and bands; B. The statistical analysis of expression of caspase-12; C. The statistical analysis of expression of CHOP; D. The statistical analysis of expression of *GRP78*; E. The statistical analysis of the ratio of p-JNK/JNK; *$p < 0.05$ compared to untreated cells group

#$p < 0.05$, ##$p < 0.01$ compared to untreated cervical cancer cells at the same time points.

Discussion

Cervical cancer is considered to be a leading cause of cancer-associated death worldwide for women.[16] It is usually diagnosed clinically as advanced or moderate stages; however, the efficacy of traditional therapy is relatively poor.[17] Therefore, there is a significant and urgent need to establish an effective and safe therapeutic strategy for cervical cancer. Although USI could induce apoptosis in both cancer cells and normal cells, the cancer cells are more sensitive to the treatment and more easily killed compared to normal cells.[18,19] Meanwhile, Lagneaux et al.[20] reported that cancer cells are more susceptible to the USI due to higher cell apoptotic rates. Therefore, USI that can cause apoptosis might be of clinical importance as a novel therapeutic approach.

In this study, we first examined cell viability and apoptosis in both a normal cervical cell line (HaCaT cells) and cervical cancer cell lines (C33A, Hela and Siha). The MTT assay results showed that USI significantly reduced the cell viability of all cancer cells at 6 h, 12 h and 24 h post-treatment. The flow cytometry assay findings indicated that USI triggered significant amounts of apoptosis in all cervical cancer cells at 6 h, 12 h and 24 h post-treatment. However, USI demonstrated no effects on the cell viability and apoptosis of normal cervical cells. Therefore, we believed

that USI treatment is safe for normal cervical cells, and only the cervical cancer cells were utilized in the following experiments for exploring mechanisms of cell viability and apoptosis.

Apoptosis, a process of programmed cell death, can maintain tissue homeostasis and eliminate dead cells from both normal and cancer tissues.[21] Previous studies have reported that there are 2 main categories of apoptosis, including mitochondria-mediated[22,23] and ER stress-mediated apoptosis.[14,24] Ultrasound irradiation-induced apoptosis of cancer cells has previously been demonstrated to use the mitochondria-associated pathway[25]; therefore, this aspect is not discussed. In the present study, we investigated whether USI caused apoptosis by verifying the biomarker expression of ER stress-mediated apoptosis, including *GRP78*, CHOP and caspase-12.[26] Our results showed that all of these ER stress biomarkers were significantly upregulated following USI in treated cervical cancer cells compared to untreated tumor cells. This suggests that USI induced cancer cell death (decreased cell viabilities) and apoptosis (formed apoptotic bodies) via the ER-mediated signaling pathway.

A previous study[27] demonstrated that p-JNK is associated with cell apoptosis, and therefore we also evaluated the levels of p-JNK in USI-treated cervical cancer cells. Our results indicated that USI triggered a significant increase in p-JNK in both C33A cells and Siha cells. This result suggests that USI induced apoptosis in cervical cancer cells also via activating p-JNK, which is consistent with the previous study.[28]

The GRP78 protein plays critical roles in regulating ER-mediated apoptosis in cancer cells.[29] When cancer cells are suffering from the stimuli, *GRP78* is overexpressed to regulate any misfolded proteins, and in this way, silencing of the *GRP78* gene might initiate ER stress.[30] In this study, we designed the siRNA sequence of *GRP78*-homo-1548 to downregulate *GRP78* expression and to clarify the role of this key molecule in USI-mediated apoptosis. The results indicated that silencing of *GRP78* significantly upregulated caspase-12 and CHOP expression, which increases ER stress-mediated apoptosis of Hela cells. Meanwhile, p-JNK expression was also activated in Hela cells undergoing *GRP78* silencing. These findings suggest that the *GRP78* molecule might participate in apoptosis in USI-treated cervical cancer cells.

Limitations

Although this study received a few interesting findings, there are also some limitations.

This study mainly focused on ER stress-induced apoptosis; however, we did not discuss the classical apoptosis pathway. Actually, some previous studies[31–34] have explored the classical pathways or molecules involved in USI-induced apoptosis of cancer cells. Xu et al.[31] reported that ultrasound could induce apoptosis in cervical cancer cells via regulating Bcl-2 and Bax proteins. Xiao et al.[32] found that ultrasound demonstrated a wider application in the clinical treatment of cervical cancer through modulating cleaved caspase-9. Chen et al.[33] proved that ultrasound remarkably downregulated Bax and caspase-3 expression in cervical cancer cells. Finally, Tang et al.[34] discovered that caspase-8 is also involved in the apoptosis in ultrasound-treated cancer cells. However, the intrinsic apoptosis pathway (involving tumor necrosis factor α (TNF-α), TRAIL and FAS-L molecule) and extrinsic apoptosis pathway (involving mitochondria-mediated molecules) have not been fully clarified herein, which is a limitation of our study.

Conclusions

The present findings indicated that USI could significantly inhibit the proliferation and induce apoptosis of cervical cancer cells. Ultrasound irradiation-induced cervical cell apoptosis was mediated by initiating the ER stress-associated signaling pathway and triggering the phosphorylation of JNK in cervical cancer cells. These results might provide the experimental insight for the therapeutic intervention of USI in cervical cancer therapy. In the future, we would investigate the effects of USI on tumor growth of xenografted mice. Moreover, we would also combine USI and ER stress inducers for enhancing the regression of tumors with the minimum off-target effects.

ORCID iDs

Juan Qin https://orcid.org/0000-0002-1358-1663
Guolin Song https://orcid.org/0000-0001-7104-2708
Qin Liu https://orcid.org/0000-0003-2243-7839
Hong Lin https://orcid.org/0000-0001-9968-1405
Yan Wang https://orcid.org/0000-0003-1984-7597
Jinyun Chen https://orcid.org/0000-0002-6818-7145

References

1. Siegel RL, Miller KD, Jemal A. Cancer statistics, 2017. *CA Cancer J Clin*. 2017;67(1):7–30. doi:10.3322/caac.21387
2. Zielecka-Debska D, Blaszczyk J, Blaszczyk D, et al. The effect of the population-based cervical cancer screening program on 5-year survival in cervical cancer patients in Lower Silesia. *Adv Clin Exp Med*. 2019;28(10):1377–1383. doi:10.17219/acem/109759
3. Feraly J, Shin HR, Bray F, Forman D, Mathers C, Parkin DM. Estimates of worldwide burden of cancer in 2008: GLOBOCAN 2008. *Int J Cancer*. 2010;127(12):2893–2917. doi:10.1002/ijc.25516
4. Bhat S, Kabekkodu SP, Noronha A, Satyamoorthy K. Biological implications and therapeutic significance of DNA methylation regulated genes in cervical cancer. *Biochimie*. 2016;121:298–311. doi:10.1016/j.biochi.2015.12.018
5. Fulda S, Debatin KM. Apoptosis pathways in neuroblastoma therapy. *Cancer Lett*. 2003;197(1–2):131–135. doi:10.1016/s0304-3835(03)00091-0
6. Wang SY, Li Y, Jiang YS, Li RA. Investigation of serum miR-411 as a diagnosis and prognosis biomarker for non-small cell lung cancer. *Eur Rev Med Pharmacol Sci*. 2017;21(18):4092–4097. PMID:29028091
7. Feril LB, Kondo T, Zhao QL, et al. Enhancement of ultrasound-induced apoptosis and cell lysis by echo-contrast agents. *Ultrasound Med Biol*. 2003;29(2):331–337. doi:10.1016/s0301-5629(02)00700-7
8. Yu T, Wang Z, Mason TJ. A review of research into the uses of low level ultrasound in cancer therapy. *Ultrason Sonochem*. 2004;11(2):95–103. doi:10.1016/S1350-4177(03)00157-3

9. Tian ZM, Wan MX, Lu MZ, Wang XD, Wang L. The alteration of protein profile of Walker 256 carinosarcoma cells during the apoptotic process induced by ultrasound. *Ultrasound Med Biol*. 2005;31(1):121–128. doi:10.1016/j.ultrasmedbio.2004.09.008
10. Liu B, Luo Y, Luo D, et al. Treatment effect of low intensity pulsed ultrasound on leukopenia induced by cyclophosphamide in rabbits. *Am J Transl Res*. 2017;9(7):3315–3325. PMID:28804549
11. Shi M, Liu B, Liu G, et al. Low intensity-pulsed ultrasound induced apoptosis of human hepatocellular carcinoma cells in vitro. *Ultrasounds*. 2016;64:43–53. doi:10.1016/j.ultras.2015.07.011
12. Yang F, Yu X, Li T, et al. Exogenous H_2S regulates endoplasmic reticulum-mitochondria cross-talk to inhibit apoptotic pathways in STZ-induced type I diabetes. *Am J Physiol Endocrinol Metab*. 2017;312(3): E199–E203. doi:10.1152/ajpendo.00196.2016
13. Wang L, Zhang M, Tan K, Kim S, Lee SH. Preparation of nanobubbles carrying androgen receptor siRNA and their inhibitory effects on androgen-independent prostate cancer combined with ultrasonic irradiation. *PLoS One*. 2014;9(5):e96586. doi:10.1371/journal.pone.0096586
14. Yun S, Han YS, Lee JH. Enhanced susceptibility to 5-fluorouracil in human colon cancer cells by silencing *GRP78*. *Anticancer Res*. 2017; 37(6):2975–2984. doi:10.21873/anticanres.11651
15. Zou L, Li X, Wu N, Jia P, Liu C, Jia D. Palmitate induces myocardial lipotoxic injury via the endoplasmic reticulum stress-mediated apoptosis pathway. *Mol Med Rep*. 2017;16(5):6934–6939. doi:10.3892/mmr.2017.7404
16. Einstein MH, Schiller JT, Viscidi RP, et al. Clinician's guide to human papillomavirus immunology: Knowns and unknowns. *Lancet Infect Dis*. 2009;9(6):347–356. doi:10.1016/S1473-3099(09)70108-2
17. Heijkoop ST, Nout RA, Quint S, Mens JWM, Heijmen BJM, Hoogeman MS. Dynamics of patient reported quality of life and symptoms in the acute phase of online adaptive external beam radiation therapy for locally advanced cervical cancer. *Gynecol Oncol*. 2017;147(2):439–449. doi:10.1016/j.ygyno.2017.08.009
18. Feng Y, Tian ZM, Wan MX, Zheng ZB. Low intensity ultrasound-induced apoptosis in human gastric carcinoma cells. *World J Gastroenterol*. 2008;14(31):4873–4879. doi:10.3748/wjg.14.4873
19. Li H, Liu J, Chen M. Therapeutic evaluation of radiotherapy with contrast-enhanced ultrasound in non-resectable hepatocellular carcinoma patients with portal vein tumor thrombosis. *Med Sci Monit*. 2018;24:8183–8189. doi:10.12659/MSM.911073
20. Lagneaux L, de Meulenaer EC, Delforge A, et al. Ultrasound low-energy treatment: A novel approach to induce apoptosis in human leukemic cells. *Exp Hematol*. 2002;30(11):1293–1301. doi:10.1016/s0301-472x(02)00920-7
21. Wang Q, Xu H, Zhao X. Baicalin inhibits human cervical cancer cells by suppressing protein kinase C/signal transducer and activator of transcription (PKC/STAT3) signaling pathway. *Med Sci Monit*. 2018; 23:1955–1961. doi:10.12659/msm.909640
22. Huang LH, Li J, Gu JP, Qu MX, Yu J, Wang ZY. Butorphanol attenuates myocardial ischemia reperfusion injury through inhibiting mitochondria-mediated apoptosis in mice. *Eur Rev Med Pharmacol Sci*. 2018;22(6):1819–1824. doi:10.26355/eurrev_201803_14601
23. Zhang H, Zhang Y, Hu S. Melatonin protects cardiac microvasculature against ischemia/reperfusion injury via suppression of mitochondrial fission–VDAC1–HK2–mPTP–mitophagy axis. *J Pineal Res*. 2017;63(1):12413. doi:10.1111/jpi.12413
24. Zhu P, Hu S, Jin Q. Ripk3 promotes ER-stress-induced necroptosis in cardiac IR injury: A mechanism involving calcium overload/XO/ROS/mPTP pathway. *Redox Biol*. 2018;16:157–168. doi:10.1016/j.redox.2018.02.019
25. Xu XM, Zhang Y, Qu D, Jiang TS, Li SQ. Osthole induces G2/M arrest and apoptosis in lung cancer A549 cells by modulating PI3K/Akt pathway. *J Exp Clin Cancer Res*. 2011;30(1):33. doi:10.1186/1756-9966-30-33
26. Yin ZC, Xiong WH, Pang QJ. CXCR3 mediates chondrocyte injury through regulating nitric oxide. *Eur Rev Med Pharmacol Sci*. 2018;22(8): 2454–2460. doi:10.26355/eurrev_201804_14839
27. Nadel G, Yao Z, Ben-Ami I, Naor Z, Seger R. Gg-induced apoptosis is mediated by AKT inhibition that leads to PKC-induced JNK activation. *Cell Physiol Biochem*. 2018;50(1):121–135. doi:10.1159/000493963
28. Deng B, Zhang S, Miao Y, Wen F, Guo K. Down-regulation of Frizzled-7 expression inhibits migration, invasion and epithelial-mesenchymal transition of cervical cancer cell lines. *Med Oncol*. 2015;32(4):102. doi:10.1007/s12032-015-0552-8
29. Luo C, Fan W, Jiang Y, Zhou S, Cheng W. Glucose-related protein 78 expression and its effects on cisplatin-resistance in cervical cancer. *Med Sci Monit*. 2018;23:2197–2209. doi:10.12659/MSM.906413
30. van Lidth de Jeude JF, Meijer BJ, Wielenga MCB, et al. Induction of endoplasmic reticulum stress by deletion of Grp78 depletes Apc mutant intestinal epithelial stem cells. *Oncogene*. 2017;36(24):3397–3405. doi:10.1038/onc.2016.326
31. Xu T, Nie Y, Bai J, et al. Suppression of human 8-oxoguanine DNA glycosylase (OGG1) augments ultrasound-induced apoptosis in cervical cancer cells. *Ultrasonics*. 2016;72:1–14. doi:10.1016/j.ultras.2016.07.005
32. Xiao X, Zhang Y, Lin Q, Zhong K. The better effects of microbubble ultrasound transfection of miR-940 on cell proliferation inhibition and apoptosis promotion in human cervical cancer cells. *Onco Targets Ther*. 2019;12:6813–6824. doi:10.2147/OTT.S209692
33. Chen ZY, Liang K, Lin Y, Yang F. Study of the UTMD-based delivery system to induce cervical cancer cells apoptosis and inhibit proliferation with shRNA targeting survivin. *Int J Mol Sci*. 2013;14(1):1763–1777. doi:10.3390/ijms14011763
34. Tang W, Liu Q, Wang X, et al. Involvement of caspase 8 in apoptosis induced by ultrasound-activated hematoporphyrin in sarcoma 180 cells in vitro. *J Ultrasound Med*. 2009;27(4):645–656. doi:10.7863/jum.2008.27.4.645